RSC Advances

PAPER

View Article Online
View Journal | View Issue

Cite this: *RSC Adv.*, 2023, **13**, 35621

Effect of nano-Al_2O_3 and multi-walled carbon nanotubes on the anaerobic mono-digestion of sludge and the co-digestion of tobacco waste and sludge

Hongmei Zhao, †[ab] Shibo Cheng,†[a] Congqi Zhao,[c] Kejiang Ruan,[b] Junju Xu*[c] and Xiaohong Cheng*[a]

Received 21st October 2023
Accepted 1st December 2023

DOI: 10.1039/d3ra07170g

rsc.li/rsc-advances

Anaerobic digestion can help mitigate tobacco waste (TW) pollution. Both the mono-digestion of sludge and the co-digestion of TW and sludge were considered in this study. Additionally, the effects of nano-Al_2O_3 and multi-walled carbon nanotubes (MWCNTs) on these two digestion systems were investigated through a 35 day digestion experiment. The microbial communities in the control reactors and the nano-Al_2O_3 reactors were also examined. Kinetic analysis revealed that the R_m values for the mono- and co-digestion nano-Al_2O_3 reactors increased by 8.88% and 13.5% compared with that of the MWCNTs reactor, respectively. Furthermore, the co-digestion system exhibited a 34.8% higher R_m than the mono-digestion system when nano-Al_2O_3 was added to both systems. Nano-Al_2O_3 was found to shorten the lag phase, while MWCNTs prolonged the lag phase time. Furthermore, 16S RNA amplicon sequencing results indicated that microbial species such as *Methanobacterium* sp., *Hydrogenispora* sp., *Lutispora* sp., and *Ruminiclostridium* sp. were more abundant in the nano-Al_2O_3 reactor. These results demonstrated that biogas production in co-digestion systems was improved. Moreover, nano-Al_2O_3 addition enhanced biogas production.

1 Introduction

Tobacco, as an important non-edible economic crop, and has been widely cultivated in many countries.[1,2] A lot of tobacco waste (TW) is produced every year.[3] TW is harmful to the environment, and it is usually incinerated, pyrolyzed, composted, or sent to landfills.[4,5]

Anaerobic digestion (AD) is the most effective renewable and sustainable method to convert waste into biomass energy. There are several advantages of AD: (1) it is characterized by a high organic loading rate, high treatment efficiency, and low sludge growth rate; (2) it can convert organic matter in waste into biogas; and (3) biogas slurry and residues from AD are valuable fertilizers in agriculture.[6–9] Owing to these benefits, some researchers have focused on AD. In recent years, the conversion of TW into biomass energy through AD has been studied. Liu *et al.* obtained the maximum methane yield of 0.163 m^3 CH_4 per kg VS from co-digestion of tobacco stalks, wheat stalks and pig manure.[9] González-González *et al.* obtained a methane yield of 53.84 ± 14.48 Nm^3 CH_4 per t from fresh tobacco under mesophilic conditions with a degradation period of 16 days.[10,11] Ye *et al.* studied the cellulose content of TW, and the results showed that TW was suitable for AD owing to its lower cellulose content.[12]

However, TW is characterized by a typical lignocellulosic structure and lower biodegradability during the AD process.[9] Moreover, AD could be inhibited because TW also has a higher alkaloid nicotine content. For example, the effect of nicotine on AD was investigated by Wang *et al.*[13] They found that methane production decreased when nicotine content was added to the systems.[13] According to a previous study, nicotine mainly affected microbial growth. To improve methane production and enhance microbial activity, some researchers have added additives, particularly nanomaterials additives, to the AD systems for TW. He *et al.* added biochar to the AD of flue-cured TW and studied its effects. Biochar enhanced methane production and shortened the lag period.[14] This finding suggests that biochar can promote direct interspecific electron transfer.[15–21] This interesting discovery provides an important reference for the AD process of TW. However, no studies have focused on the effects of other nanoporous materials, such as nano-Al_2O_3 or multi-walled carbon nanotubes (MWCNTs), on the co-digestion of TW and sludge.

[a]*Key Laboratory of Medicinal Chemistry for Natural Resource, Ministry of Education, Yunnan Research & Development Center for Natural Products, School of Chemical Science and Technology, Yunnan University, Kunming 650091, China. E-mail: xhcheng@ynu.edu.cn*

[b]*College of Science, Yunnan Agricultural University, Kunming, 650201, China*

[c]*College of Tobacco Science, Yunnan Agricultural University, Kunming 650201, China. E-mail: junjuxu007@126.com*

† Both authors contributed equally to this work.

Table 1 TS and VS of waste tobacco and sludge

Raw materials	TS (%)	VS (%)
Tobacco waste	90.17 ± 0.25	77.0 ± 2.59
Sludge	44.07 ± 7.51	77.87 ± 3.45

Therefore, in this study, the changes in biogas production and microbial community from air-cured tobacco leaf waste and sludge using a dry AD system were investigated. To improve biogas production, the effects of nano-Al_2O_3 and MWCNT addition on AD performance were studied. The purposes of this study were as follows: (a) to compare biogas production, coenzyme F_{420} activities, chemical oxygen demand (COD) concentrations, and volatile fatty acid (VFA) concentrations during the dry AD process, and to explain the effects of two nanomaterials in mono-digestion and co-digestion systems; (b) to investigate the microbial community structure when nano-Al_2O_3 was added to the mono-digestion system and the co-digestion system.

2 Materials and methods

2.1 Materials

The TW used in the experiment was obtained from Yunnan Agricultural University, Yunnan Province. The samples were cut into small pieces (1–2 cm). The dehydrated sludge was collected from the Fifth Water Purification Plant in Kunming, Yunnan Province, and it appeared brown in color. The total solid (TS) content and the volatile solid (VS) content of tobacco were tested (Table 1). The C/N ratio of tobacco is presented in Table 2. The C/N ratio of TW was relatively low, and this ratio plays an important role in the AD process.[22] According to the literature, a low C/N ratio can restrict VFA generation.[25] C/N ratios between 20% and 30% are considered appropriate.[23]

2.2 Experimental setup

The experimental setup and the synthesis of nano-Al_2O_3 were based on our previous research.[26] We set up six dry AD reactors: three reactors with sludge (the control [C], 300 mg per kg Al_2O_3 [CA], 300 mg per kg MWCNTs [CC]) and three reactors with TW and sludge (the control [CT], 300 mg per kg Al_2O_3 [CTA], 300 mg per kg MWCNTs [CTC]). All experiments were conducted at (35 ± 1) °C for 35 days (Table 3).

2.3 Analytical methods

The pH was measured using a pH meter (OHAUS, ST2100C), and the COD values were determined with a water quality rapid tester (5B-6CU8.3). TS and VS were measured following standard methods.[25] The analytical method for F_{420} has been described in the literature.[26] Total carbon and total nitrogen were measured using an elemental analysis instrument (VARIO EL 3, Germany). VFAs were tested using standard methods.[27,28]

Table 2 Elemental content analysis of TW

	Element content		
Raw materials	C (%)	N (%)	C/N (%)
Tobacco waste	37.20 ± 0.092	3.30 ± 0.021	11.26 ± 0.05
Sludge	36.51 ± 0.08	0.74 ± 0.01	49.33 ± 0.045

Table 3 Design of experiments in dry AD systems

Reactors	Tobacco waste (g)	Sludge (g)	Water (g)	Amount of additives (mg kg^{-1})
C	0	20	200	0
CA	30	20	200	300
CC	30	20	200	300
CT	0	20	200	0
CTA	30	20	200	300
CTC	30	20	200	300

2.4 Kinetic analysis

The modified Gompertz was used to fit the measured biogas production. The modified Gompertz was as follow:[29,30]

$$P = P_m \exp(-\exp(R_m e/P_m(\lambda - t) + 1))$$

where "P" is the cumulative biogas production at time, "P_m" is the maximum cumulative biogas production. "R_m" is the maximum biogas rate (mL d^{-1} g^{-1}), "e" is Euler's number (2.71828), "λ"is the lag phase time (d), and t is infinite digestion time (t).

2.5 Microbial community analysis

The test steps were as follows: first, DNA was extracted from 12 samples using the MIO-BIO Power Soil DNA Isolation Kit. Second, polymerase chain reaction (PCR) primers were designed, and the product was recovered. The V4–V5 variable region of the bacterial 16S rRNA gene was amplified using primers 515F (5′-GTGCCAGCMGCCGCGGTAA-3′) and 926R (5′-CCGTCAATTCMTTTGAGTTT-3′). The archaeal 16S rRNA gene was amplified using primers Arch519F (5′-CAGCCGCCGCGGTAA-3′) and Arch915R (5′-GTGCTCCCCCGCCAATTCCT-3′). The 16S V4–V5 PCR system was as follows: 5× PCR buffer 10 μL, dNTP 1 μL, DNA polymerase 1 μL, primer (F/R) 1 μL, template DNA 5–50 ng. The PCR conditions were as follows: 2 min at 94 °C, followed by 22 cycles of 30 s at 94 °C, 30 s at 55 °C, and 30 s at 72 °C, followed by a 5 min final extension at 72 °C. The archaeal PCR system was the same as the 16S V4–V5 PCR system. The PCR conditions were as follows: 2 min at 94 °C, followed by 27 cycles of 30 s at 94 °C, 30 s at 55 °C, and 30 s at 72 °C, followed by a 5 min final extension at 72 °C. Finally, the PCR results were analyzed through high-throughput sequencing using the NGS Illumina platform.

3 Results and discussion

3.1 Effect of the two nanomaterials on AD

3.1.1 AD performance of the single sludge reactors. The daily biogas production and the cumulative biogas production

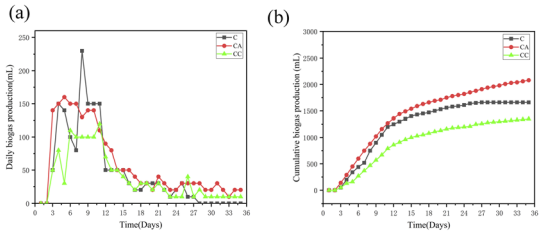

Fig. 1 Effect of daily biogas yield (a) and cumulative biogas production (b) in single sludge reactors (C: control reactor; CA: nano-Al_2O_3 reactor; CC: MWCNTs reactor).

in three reactors were shown in Fig. 1. pH is an important factor affecting acid production and in retaining methanogenesis activity. The pH values in all systems remained in the range of 6.5–7.5 throughout the entire dry AD process. The daily biogas production and the cumulative biogas production in the CA reactor were noticeably higher than those in the other reactors (C and CC reactors). This illustrated that nano-Al_2O_3 can improve the biogas production of active sludge, while biogas production was suppressed with the addition of MWCNTs.

3.1.2 Performance of co-digestion reactors. As shown in Fig. 2, the daily biogas production and the cumulative biogas production in the co-digestion reactors were higher than those in the single sludge reactors. The largest daily biogas production was 760.00 mL when nano-Al_2O_3 was added. Moreover, the biogas production reached its peak on day 2. After day 15 and day 24, another small peak occurred. The largest daily biogas production for the second peak also came from the nano-Al_2O_3 reactor (CTA, 180 mL). From day 24, a third peak appeared. The daily biogas production in the CTA reactor was lower than that in the CT and CTC reactors. The effect of nano-Al_2O_3 on methanogenic activity possibly became smaller in the later stages of the AD process. The cumulative biogas production in the CTA reactor (7310 mL) was higher than that in the CTC reactor (4890 mL). The results illustrate that nano-Al_2O_3 can improve biogas production in TW and sludge co-digestion systems. As in previous research, nano-Al_2O_3 has no toxic effects on the methanogenic activity and can provide a good carrier for the AD process.[24,31,32]

As discussed above, the cumulative biogas production in co-digestion systems was higher than that in mono-digestion systems. Nano-Al_2O_3 enhanced biogas production, while MWCNTs inhibited it.

3.1.3 Coenzyme F_{420}. Coenzyme F_{420}, also known as 8-hydroxy-5-deazaflavin, is a low-potential electron carrier and an important enzyme found in methanogens.[33] It can be used to reflect methanogenic activity.[34–36] Fig. 3 illustrates the variations in coenzyme F_{420} activities. In mono-digestion systems, the coenzyme F_{420} activity increased during the first 15 days in the group with nano-Al_2O_3, while it decreased in the group with MWCNTs. This result shows that the addition of nano-Al_2O_3 improved the coenzyme F_{420} activity at the start of the experiment. In the co-digestion systems, no significant difference in coenzyme F_{420} levels existed between the groups with nano-Al_2O_3 and MWCNTs throughout the entire AD process. In the nano-Al_2O_3-containing group, the coenzyme F_{420} activity increased during the first 18 days, while in the MWCNT-added group, it initially increased and then decreased after day 9.

3.1.4 Variations in COD concentration during the dry AD process. The variations in COD concentration are shown in Fig. 4. In contrast to the results of previous research, the COD concentration fluctuated significantly. In a previous study, during the AD process, the COD content was the outcome of the balance between hydrolysis, acetogenesis, and methanogenesis stages.[37] The COD concentration have changed with different AD time. From the 3rd to the 9th day of the AD, the COD concentration in the CA and CTA reactors were lower, corresponding to the increase of cumulative and daily biogas yields

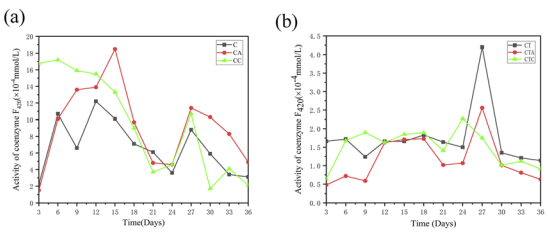

Fig. 3 Variation in coenzyme F_{420} activity in single sludge systems (a) (C: control reactor; CA: nano-Al_2O_3 reactor; CC: MWCNTs reactor) and co-digestion systems (b) (CT: control reactor; CTA: nano-Al_2O_3 reactor; CTC: MWCNTs reactor).

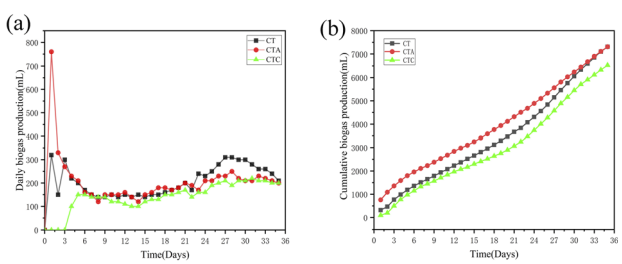

Fig. 2 Effect of daily biogas yield (a) and cumulative biogas production (b) in co-digestion sludge reactors (CT: control reactor; CTA: nano-Al_2O_3 reactor; CTC: MWCNTs reactor).

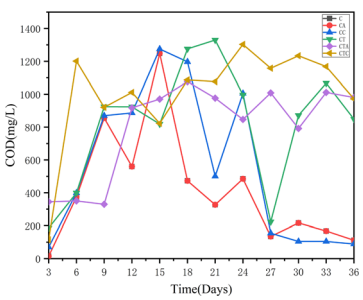

Fig. 4 Changes in COD concentration in different reactors (in mono-digestion C: control reactor; CA: nano-Al_2O_3 reactor; CC: MWCNTs reactor; in co-digestion CT: control reactor; CTA: nano-Al_2O_3 reactor; CTC: MWCNTs reactor).

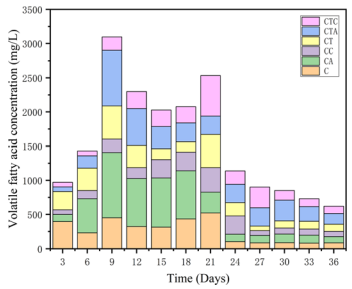

Fig. 5 Changes in VFA concentrations during the AD process in different reactors.

(Fig. 4). This illustrated that organic components in two systems have been efficiently use to produce biogas.[37]

3.1.5 Responses of volatile fatty acids. Volatile fatty acids (VFAs) are intermediate products in the methanogenic process of anaerobic digestion and are a key factor in the smooth progress of AD. A sequence of complex biochemical reactions leads to the accumulation of fatty acids during the dry AD process. Fig. 5 illustrates the concentration changes of VFAs in different reactors. In both mono- and co-digestion systems, the VFA concentration in the C and CT reactors increased rapidly in the early stages of digestion, especially in the C reactors. The accumulation of VFAs can lead to the reduction of biogas production.[38] In the middle stages of AD (from day 15 to day 21), the VFA concentration was significantly lower in the CTA reactor. Trophic methane bacteria acetate can join in the intermediate transfer of acetic acid. Acetic acid can reduce fatty acid accumulation and the high-activity H_2 trophic methane bacteria can promote the degradation of VAFs.[39] It was speculated that the methanogenic archaea in the nano-Al_2O_3 systems were mainly the acetate trophic and H_2 trophic. The microbial analysis would confirm this suspicion.

3.2 Kinetic study of cumulative biogas production

The Gompertz model was selected to fit cumulative biogas production, and the parameters of the Gompertz model are presented in Table 4. As shown in Table 4, the fitting based on the Gompertz equation resulted in R^2 values within the range of 0.95–0.99, indicating an effective fit of the Gompertz equation.

Thus, the AD process can be accurately simulated. The cumulative biogas production (P) is an important parameter used to evaluate biogas production. The P values for the six reactors were as follows: 1642.28401 ± 10.2682 mL (control, C, mono-digestion), 1973.6793 ± 22.7508 mL (nano-Al_2O_3, CA, mono-digestion), 1718.3792 ± 23.2571 mL (MWCNTs, CC, mono-digestion), 7310.0000 ± 0 mL (control, CT, co-digestion), 8230.6428 ± 1044.7869 mL (nano-Al_2O_3, CTA, co-digestion), and 4890.0000 ± 0 mL (MWCNTs, CTC, co-digestion). The order of the P values was as follows: CTA > CT > CTC > CA > CC > C. The R_m values for the mono- and co-digestion nano-Al_2O_3 reactors increased by 8.88% and 13.5% compared with that of the MWCNT reactor, respectively. Moreover, the R_m values of the co-digestion system increased by 34.8% compared with that of the mono-digestion system when nano-Al_2O_3 was added to both systems. This further illustrates that nano-Al_2O_3 had a positive impact on both co-digestion and mono-digestion systems. The lag phase time (λ) can also indicate biogas production. The value of λ was lower in the nano-Al_2O_3-added groups. The results indicated that the lag time was reduced and the reaction rate was improved when nano-Al_2O_3 was added to both systems.

3.3 Microbial community

3.3.1 Alpha-diversity and beta-diversity analysis. Considering the positive effects on the AD process, the microbial communities of the control reactors and the nano-Al_2O_3 reactors were selected for analysis. The four alpha-diversity indices (Chao1, ACE, Shannon, and Simpson) are presented in Table 5. In mono-digestion systems, the Chao1, ACE, and Shannon indices of the bacterial community of the CA reactor were higher than those of the CC reactor. This indicates that the bacterial community was richer in the CA group. For archaea, the order of the Chao1, ACE, and Shannon indices was the same as the order of the bacterial community; that is, CA exhibited higher bacterial and archaeal diversities. The Simpson index of the bacterial and archaeal communities in CA was lower, suggesting that the addition of nano-Al_2O_3 can increase the relative abundance of dominant flora. A comparison of the co-digestion system with the mono-digestion system revealed that the Chao1, ACE, and Shannon indices of the bacterial community in the CTA reactor were lower than those of the CT reactor. The order of the Chao1, ACE, and Shannon indices for archaea was the same as the order for the bacterial community. However, the Simpson index for archaea in CTA was lower. This indicates that nano-Al_2O_3 addition mainly influenced the succession of archaea in the co-digestion system.

Table 4 Modified Gompertz model parameters of the cumulative biogas production in different reactors

Reactors	P^a	$R_m{}^b$	λ^c	R^{2d}
C	1642.2840 ± 10.2682	149.084 ± 4.6235	3.0344 ± 0.1783	0.995
CA	1973.6793 ± 22.7508	135.128 ± 5.9486	1.7794 ± 0.3252	0.988
CC	1718.3792 ± 23.2571	122.628 ± 6.1098	3.6927 ± 0.3509	0.988
CT	7310.0000 ± 0	218.739 ± 12.492	2.7250 ± 0.9558	0.951
CTA	8230.6428 ± 1044.7869	207.141 ± 15.858	−0.7999 ± 1.2377	0.977
CTC	4890.0000 ± 0	187.406 ± 7.790	7.7901 ± 0.6653	0.971

[a] Cumulative biogas production. [b] Maximum biogas production. [c] Lag phase time. [d] Correlation coefficients.

Table 5 Indices of alpha diversity of archaeal and bacterial communities during the AD process

	Chao1		ACE		Shannon's		Simpson's	
Reactors	Bacterial	Archaeal	Bacterial	Archaeal	Bacterial	Archaeal	Bacterial	Archaeal
C	2097.3920	64.7333	2127.0200	65.22086	5.5608	2.6572	0.01320	0.1109
CA	2137.0080	87.8846	2159.3540	88.8773	5.7024	2.8564	0.01009	0.08937
CT	2155.7780	93.7321	2175.6990	92.7387	5.6066	2.5088	0.01011	0.1966
CTA	1838.9040	89.5214	1858.5450	91.1168	5.1785	2.3526	0.02278	0.1631

Beta diversity represents the differences in species composition between different reactors. As shown in Fig. 6, principal coordinate analysis (PCoA) illustrates the variations in microbial community composition. The contribution rates of principal components 1 and 2 were 15.51% and 14.38%, respectively. The first and second ordination axes could explain 79.24% and 15.37% of the archaeal community, respectively. Similarly, they could account for 40.6% and 10.69% of the bacterial community, respectively. As shown in Fig. 6, the C and CA reactors were notably separated from the CT and CTA reactors in the PCoA plot. These results indicate that the microbial community structure in mono-digestion and co-digestion systems differs significantly. Furthermore, the nano-Al_2O_3 reactors were distinctly separated from the control reactors in the bacterial PCoA plot (Fig. 6(b)), showing significant differences in bacterial community structure between the nano-Al_2O_3 reactors and the control reactors. Therefore, the addition of nano-Al_2O_3 had a pronounced effect on microbial diversity, richness, and composition during the AD process.

3.3.2 Analysis of microbial species. For a more in-depth analysis of the effects of nano-Al_2O_3 addition on microbial community structure, archaeal and bacterial species at the phylum and genus levels were investigated. As shown in Fig. 7(a), there were three phyla: *Euryarchaeota*, *Thaumarchaeota*, and *Crenarchaeota*. *Euryarchaeota* was the dominant phylum, accounting for 99% of the relative abundance in all reactors. The relative abundance of *Crenarchaeota* was smaller. Studies have shown that *Crenarchaeota* played a key role in ammonia oxidation.[40,41] The results indicated that the addition of nano-Al_2O_3 did not enhance the activity of *Crenarchaeota*. The bacterial community consisted of 17 phyla. The dominant phyla were Firmicutes, Bacteroidetes, Proteobacteria, Chloroflexi, and Synergistetes. Studies have demonstrated that these dominant phyla are primarily involved in the degradation of organic matter (such as proteins, lignocellulose, and fats).[42–44] In mono-digestion systems, the nano-Al_2O_3 reactor exhibited a higher relative abundance of Bacteroidetes than the control reactor. Nano-Al_2O_3 addition may promote the hydrolysis of polysaccharides owing to the effect of Bacteroidetes in hydrolyzing polysaccharides.[45] In co-digestion systems, Firmicutes showed a significant increase in the nano-Al_2O_3 reactor compared with mono-digestion systems. Firmicutes are an important microbial community with many significant functional microorganisms.[46] In summary, nano-Al_2O_3 had a positive effect on the microbial community. Fig. 7(c) and (d) show the heat maps of archaeal and bacterial genera in different AD systems. The top four archaeal genera were *Methanobacterium* sp., *Methanosarcina* sp., *Methanosaeta* sp., and *Methanospirillum* sp. Co-digestion resulted in a higher relative abundance of *Methanobacterium* sp. and *Methanosarcina* sp. than mono-digestion. *Methanobacterium* sp. played an important role in the AD process. *Methanosarcina* sp. is a type of methanogen that produces acetic acid. This suggests that the activities of *Methanobacterium* sp. and *Methanosarcina* sp. could be enhanced in co-digestion. Moreover, the relative abundance of *Methanobacterium* sp. in the nano-Al_2O_3 reactor was higher than that in the corresponding control reactor. Nano-Al_2O_3 addition resulted in an increase in the relative abundance of *Methanosarcina* sp. but a decrease in that of *Methanosaeta* sp. These results indicated that *Methanosarcina*

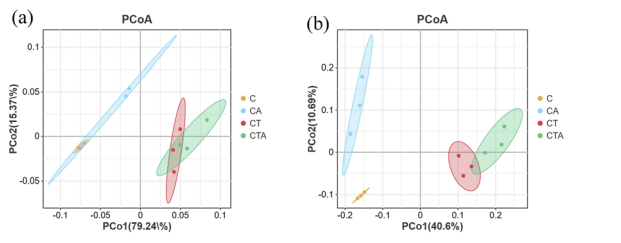

Fig. 6 Archaeal (a) and bacterial (b) PCoA; differently colored points represent different groups (orange: C; blue: CA; red: CT; green: CTA).

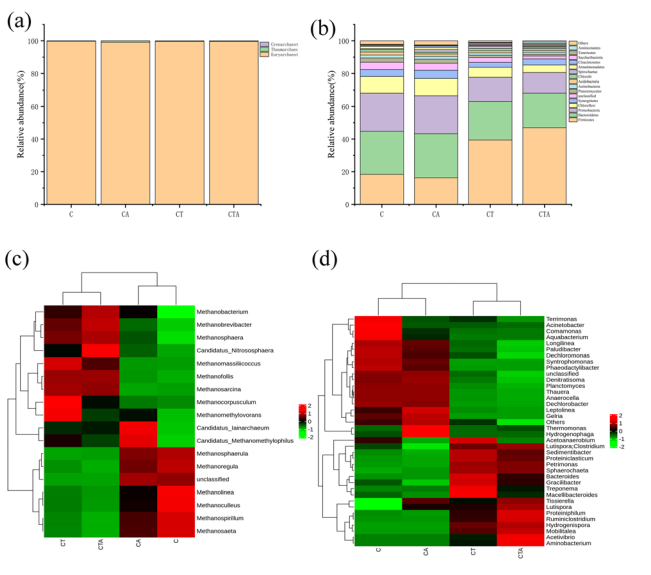

Fig. 7 Archaeal (a) and bacterial community (b) structure at the phylum level. The heat map of the top 18 archaea (c) and 38 bacteria (d) at the genus level in the four reactors during the dry AD process.

sp. and *Methanosaeta* sp. have a competitive relationship.[45] As shown in Fig. 7(d), the dominant bacterial genera in all four groups were *Hydrogenispora* sp., *Lutispora* sp., *Syntrophomonas* sp., *Longilinea* sp., *Hydrogenispora* sp., and *Ruminiclostridium* sp. *Hydrogenispora* sp., *Lutispora* sp., and *Ruminiclostridium* sp. were more abundant in the CTA reactor. *Hydrogenispora* sp. and *Lutispora* sp. belong to the Firmicutes phylum and are known to be responsible for the degradation of cellulose and proteins in the AD process.[47,48] From the above discussion, it can be seen that nano-Al_2O_3 addition influenced the abundance and structure of the microbial flora.

4 Conclusions

Biogas production in both mono-digestion and co-digestion systems was enhanced with nano-Al_2O_3 addition to the AD process. Gompertz model analysis demonstrated that nano-Al_2O_3 nanomaterials shortened the lag phase. Microbial species such as *Methanobacterium* sp., *Hydrogenispora* sp., *Lutispora* sp., and *Ruminiclostridium* sp. were more abundant in the nano-Al_2O_3 reactor. Nano-Al_2O_3 had a positive impact on both mono-digestion and co-digestion systems. Maybe nano-Al_2O_3 have large specific areas and highly porous structure.[49] And nano-Al_2O_3 is a typical catalyst carrier, which can provide a good carrier for anaerobic medium and promote the occurrence of hydrogenation and redox.[50–53] In complex AD process, the effect of Al_2O_3 as a carrier will be further research in the future.

Author contributions

Hongmei Zhao: conceived and designed the experiments; performed the experiments; analyzed and interpreted the data; contributed reagents, materials, analysis tools or data; wrote the paper. Shibo Chen: conceived and designed the experiments; performed the experiments; analyzed and interpreted the data; contributed reagents, materials, analysis tools or data; wrote the paper. Congqi Zhao; Kejiang Ruan: performed the experiments; analyzed and interpreted the data. Xiaohong Cheng; Junju Xu: analyzed and interpreted the data; contributed reagents, materials, analysis tools or data; wrote the paper.

Conflicts of interest

There are no conflicts of interest to declare.

Acknowledgements

This work was supported by Agricultural Union Youth Program of Yunnan Provincial Science and Technology Department (2018FG001-102) and Scientific Research Fund of Yunnan Education Department (2023J0416). We thank Engineering and Research Center for Industrial Biogas Technology of Yunnan Province University. The archaeal diversity analysis was performed using the Omicshare tools, a free online platform for data analysis (**https://www.omicshare.com/tools**). We thank LetPub (**https://www.letpub.com**) for its linguistic assistance during the preparation of this manuscript.

References

1 M. M. Hossain, I. M. Scott, F. Berruti and C. Briens, A two-dimensional pyrolysis process to concentrate nicotine during tobacco leaf bio-oil production, *Ind. Crops Prod.*, 2018, **124**, 136–141.
2 Y. Liu, J. X. Dong, G. J. Liu, H. N. Yang, W. Liu, L. Wang, C. X. Kong, D. Zheng, J. G. Yang, L. W. Deng and S. S. Wang, Co-digestion of tobacco waste with different agricultural biomass feedstocks and the inhibition of tobacco viruses by anaerobic digestion, *Bioresour. Technol.*, 2015, **189**, 210–216.
3 J. T. He, N. Yao, Z. Y. Sun, F. Li, H. Q. Cai, L. F. Jin and Y. Q. Tang, Improved biogas production from tobacco processing waste via biochar-assisted thermophilic anaerobic digestion, *Ind. Crops Prod.*, 2021, **202**, 117038–117046.
4 Z. Yang, S. Zhang, L. Liu, X. Li, H. Chen, H. Yang and X. Wang, Combustion behaviours of tobacco stem in a thermogravimetric analyser and a pilot-scale fluidized bed reactor, *Bioresour. Technol.*, 2012, **110**, 595–602.
5 Q. Cheng, W. Huang, M. Jiang, C. Xu, G. Fan, J. Yan, B. Chai, Y. Zhang, Y. Zhang, S. Zhang, B. Xiao and G. Song, Challenges of anaerobic digestion in China, *Int. J. Environ. Sci. Technol.*, 2021, **18**, 3685–3696.
6 B. T. Bocher, M. T. Agler, M. L. Garcia, A. R. Beers and L. T. Angenent, Anaerobic digestion of secondary residuals from an anaerobic bioreactor at a brewery to enhance bioenergy generation, *J. Ind. Microbiol. Biotechnol.*, 2008, **35**, 321–332.
7 F. Tambone, P. Genevini, G. D'Imporzano and F. Adani, Assessing amendment properties of digestate by studying the organic matter composition and the degree of biological stability during the anaerobic digestion of the organic fraction of MSW, *Bioresour. Technol.*, 2009, **100**, 3140–3142.
8 M. C. Tomei, Modeling of anaerobic digestion of sludge, *Crit. Rev. Environ. Sci. Technol.*, 2009, **39**, 1003–1051.
9 Y. Liu, J. X. Dong, G. J. Liu, H. N. Yang, W. Liu, L. Wang, C. X. Kong, D. Zheng, J. G. Yang, L. W. Deng and S. S. Wang, Co-digestion of tobacco waste with different agricultural biomass feedstocks and the inhibition of tobacco viruses by anaerobic digestion, *Bioresour. Technol.*, 2015, **189**, 210–216.
10 A. González-González and F. Cuadros, Optimal and cost-effective industrial biomethanation of tobacco, *Renewable Energy*, 2014, **63**, 280–285.
11 A. González-González, F. Cuadros, A. Ruiz-Celma and F. López-Rodríguez, Potential application of anaerobic digestion to tobacco plant, *Fuel*, 2013, **113**, 415–419.
12 X. Ye, H. Liu, Q. Meng, S. Chen, Z. Hu, S. Sun, J. Ma and X. Yu, Comparison of chemical composition in stalks of different tobaccos, *Tob. Sci. Technol.*, 2013, 76–79, in Chinese.
13 L. G. Wang, H. Y. Zhang, G. Q. Liu, Z. Q. Dai, Y. Liu and C. Chen, Effect of nicotine inhibition on anaerobic

digestion and the co-digestion performance of tobacco stalks with different animal manures, *Process Saf. Environ. Prot.*, 2021, **146**, 377–382.

14 J. T. He, N. Yao, Z. Y. Sun, F. Li, H. Q. Cai, L. F. Jin and Y. Q. Tang, Improved biogas production from tobacco processing waste via biochar-assisted thermophilic anaerobic digestion, *Ind. Crops Prod.*, 2023, **202**, 117038.

15 C. R. Qi, R. Wang, S. M. Jia, J. Chen, Y. Y. Li, J. X. Zhang, G. X. Li and W. H. Luo, Biochar amendment to advance contaminant removal in anaerobic digestion of organic solid wastes: a review, *Bioresour. Technol.*, 2021, **341**, 125827.

16 C. H. Luo, F. Lü, L. M. Shao and P. J. He, Application of eco-compatible biochar in anaerobic digestion to relieve acid stress and promote the selective colonization of functional microbes, *Water Res.*, 2015, **68**, 710–718.

17 Q. Li, M. J. Xu, G. J. Wang, R. Chen, W. Qiao and X. C. Wang, Biochar assisted thermophilic co-digestion of food waste and waste activated sludge under high feedstock to seed sludge ratio in batch experiment, *Bioresour. Technol.*, 2018, **249**, 1009–1016.

18 S. Barua and B. R. Dhar, Advances towards understanding and engineering direct interspecies electron transfer in anaerobic digestion, *Bioresour. Technol.*, 2017, **244**, 698–707.

19 J. Ma, J. Pan, L. Qiu, Q. Wang and Z. Zhang, Biochar triggering multipath methanogenesis and subdued propionic acid accumulation during semicontinuous anaerobic digestion, *Bioresour. Technol.*, 2019, **293**, 122026.

20 S. Li, S. Harris, A. Anandhi and G. Chen, Predicting biochar properties and functions based on feedstock and pyrolysis temperature: a review and data syntheses, *J. Cleaner Prod.*, 2019, **215**, 890–902.

21 J. Pan, J. Ma, L. Zhai, T. Luo, Z. Mei and H. Liu, Achievements of biochar application for enhanced anaerobic digestion: a review, *Bioresour. Technol.*, 2019, **292**, 122058.

22 H. B. Nielsen and I. Angelidaki, Strategies for optimizing recovery of the biogas process following ammonia inhibition, *Bioresour. Technol.*, 2008, **99**, 7995–8001.

23 L. Y. Feng, Y. G. Chen and X. Zheng, Enhancement of waste activated sludge protein conversion and volatile fatty acids accumulation during waste activated sludge anaerobic fermentation by carbohydrate substrate addition: the effect of pH, *Environ. Sci. Technol.*, 2009, **43**, 4373–4380.

24 H. M. Zhao, H. P. Pu and Z. R. Yang, Study on the effect of different additives on the anaerobic digestion of hybrid *Pennisetum*: Comparison of nano-ZnO, nano-Fe_2O_3 and nano-Al_2O_3, *Heliyon*, 2023, **9**, e16313–e16323.

25 A. D. Eaton, A. E. Greenberg, L. S. Cleseri and M. A. H. Franson, *Standard Methods for the Examination of Water &Wastewater*, 1995.

26 Y. H. Cheng, S. X. Sang, H. Z. Huang, X. J. Liu and J. B. Ouyang, Variation of Coenzyme F_{420} Activity and Methane Yield in Landfill Simulation of Organic Waste, *J. China Univ. Min. Technol.*, 2007, **17**, 403–408.

27 R. H. Guan, *Studies on the Performance of an Anaerobic Baffled Reactor for Desizing Wastewater*, 2010.

28 N. Q. Ren and A. J. Wang, *Principles and Applications of Anaerobic Biotechnology*, 2004.

29 B. Shamurad, N. Gray, E. Petropoulos, S. Tabraiz, E. Membere and P. Sallis, Predicting the effects of integrating mineral wastes in anaerobic digestion of OFMSW using first-order and Gompertz models from biomethane potential assays, *Renewable Energy*, 2020, **152**, 308–319.

30 J. Gu, R. Liu, Y. Cheng, N. Stanisavljevic, L. Li, D. Djatkov, X. Y. Peng and X. M. Wang, Anaerobic co-digestion of food waste and sewage sludge under mesophilic and thermophilic conditions: Focusing on synergistic effects on methane production, *Bioresour. Technol.*, 2020, **301**, 122765.

31 Y. Yang, Q. Chen, J. D. Wall and Z. Hu, Potential nanosilver impact on anaerobic digestion at moderate silver concentrations, *Water Res.*, 2012, **46**, 1176–1184.

32 E. Kökdemir Ünşar and N. A. Perendeci, What kind of effects do Fe_2O_3 and Al_2O_3 nanoparticles have on anaerobic digestion, inhibition or enhancement?, *Chemosphere*, 2018, **211**, 726–735.

33 R. Jaenchen, P. Schönheit and R. K. Thauer, Studies on the biosynthesis of coenzyme F420 in methanogenic bacteria, *Arch. Microbiol.*, 1984, **137**, 362–365.

34 Y. Xi, Z. Chang, X. Ye, R. Xu, J. Du and G. Chen, Methane production from wheat straw with anaerobic sludge by heme supplementation, *Bioresour. Technol.*, 2014, **172**, 91–96.

35 H. Zhang, Y. Tian, L. Wang, X. Mi and Y. Chai, Effect of ferrous chloride on biogas production and enzymatic activities during anaerobic fermentation of cow dung and Phragmites straw, *Biodegradation*, 2016, **27**, 69–82.

36 Q. Jiang, H. Liu, Y. Zhang, M. H. Cui, B. Fu and H. B. Liu, Insight into sludge anaerobic digestion with granular activated carbon addition: Methanogenic acceleration and methane reduction relief, *Bioresour. Technol.*, 2021, **319**, 124131–124140.

37 Y. L. T, H. Y. Zhang, L. Zheng, S. S. Li, H. Hao and H. Huang, Effect of Zn Addition on the Cd-Containing Anaerobic Fermentation Process: Biodegradation and Microbial Communities, *Int. J. Environ. Res. Public Health*, 2019, **16**, 2998.

38 S. Y. Gu, R. J. Wang, H. G. Xing, M. Z. Yu, S. Y. Shen, L. Zhao, J. Y. Sun and Y. Li, Effects of different low temperature conditions on anaerobic digestion efficiency of pig manure and composition of archaea community, *Water Sci. Technol.*, 2022, **86**(5), 1181–1193.

39 W. F. Song, *Study on the Separation and Promotion of Low-Temperature Functional Microorganisms in Biogas Digestion*, Chinese Academy of Agricultural Sciences, Beijing, China, 2011.

40 J. I. Bueno-Lopez, J. R. Rangel-Mendez, F. Alatriste-Mondraon, F. Perez-Rodriguez, V. Hernandez-Montoya and F. J. Cervantes, Graphene oxide triggers mass transfer limitations on the methanogenic activity of an anaerobic consortium with a particulate substrate, *Chemosphere*, 2018, **211**, 709–716.

41 L. Ding, Z. Liu, M. Aggrey, C. Li, J. Chen and L. Tong, Nanotoxicity: the toxicity research progress of metal and metal- containing nanoparticles, *Mini-Rev. Med. Chem.*, 2015, **15**, 529–542.

42 Y. W. Chen, Z. H. Yang, Y. R. Zhang, Y. P. Xiang, R. Xu, M. Y. Jia, J. Cao and W. P. Xiong, Effects of different conductive nanomaterials on anaerobic digestion process and microbial community of sludge, *Bioresour. Technol.*, 2020, **304**, 123016–123026.

43 S. Gullert, Deep metagenome and metatranscriptome analyses of microbial communities affiliated with an industrial biogas fermenter, a cow rumen, and elephant feces reveal major differences in carbohydrate hydrolysis strategies, *Biotechnol. Biofuels*, 2016, **9**, 121–141.

44 W. Kim, K. H. Wang, S. G. Shin, S. Lee and S. Hwang, Effect of high temperature on bacterial community dynamics in anaerobic acidogenesis using mesophilic sludge inoculum, *Bioresour. Technol.*, 2010, **101**, S17–S22.

45 H. U. Cho, Y. M. Kim, Y. N. Choi, H. G. Kim and J. M. Park, Influence of temperature on volatile fatty acid production and microbial community structure during anaerobic fermentation of microalgae, *Bioresour. Technol.*, 2015, **191**, 475–480.

46 I. Vanwonterghem, P. D. Jensen, D. P. Ho, D. J. Batstone and G. W. Tyson, Linking microbial community structure, interactions and function in anaerobic digesters using new molecular techniques, *Curr. Opin. Biotechnol.*, 2014, **27**, 55–64.

47 W. Y. Chen, Z. H. Yang, Y. R. Zhang, Y. P. Xiang, R. Xu, M. Y. Jia, J. Cao and W. P. Xiong, Effects of different conductive nanomaterials on anaerobic digestion process and microbial community of sludge, *Bioresour. Technol.*, 2020, **304**, 123016–123026.

48 Y. Bai, R. Xu, Q. P. Wang, Y. R. Zhang and Z. H. Yang, Sludge anaerobic digestion with high concentrations of tetracyclines and sulfonamides: Dynamics of microbial communities and change of antibiotic resistance genes, *Bioresour. Technol.*, 2019, **276**, 51–59.

49 K. Chen, J. Wan, J. Lin and R. Zhou, Comparative study of three-way catalytic performance over Pd/CeO_2-ZrO_2-Al_2O_3 and Pd/La-Al_2O_3 catalysts: New insights into microstructure and thermal stability, *Mol. Catal.*, 2022, **526**, 112361–112374.

50 Z. Q. Yu, Y. Li, Y. L. Yao, Y. Y. Liu, Z. C. Sun, C. Shi, W. Wang and A. J. Wang, Highly selective hydrogenative ring-rearrangement of furfural to cyclopentanone over a bifunctional Ni3P/γ-Al_2O_3 catalyst, *Mol. Catal.*, 2022, **522**, 112239–112248.

51 S. Liang, T. Cai, J. Yuan, Q. Tong and X. J. Hu, Promoting effect of reduction-oxidation strategy on the Co_3O_4/γ-Al_2O_3 catalysts for propane total oxidation, *Mol. Catal.*, 2022, **533**, 112762–112772.

52 S. J. Park, S. H. Kang, H. K. Min, M. G. Seo, S. Kweon, M. B. Park, Y. H. Choi and J. W. Lee, Catalytic pyrolysis of HDPE over WOx/Al_2O_3: Effect of tungsten content on the acidity and catalytic performance, *Mol. Catal.*, 2022, **528**, 112439–112447.

53 J. Y. Liang, F. Y. Wang, W. Li, J. L. Zhang and C. L. Guo, Highly dispersed and stabilized Pd species on H_2 pre-treated Al_2O_3 for anthraquinone hydrogenation and H_2O_2 production, *Mol. Catal.*, 2022, **524**, 112264–112274.